Published in final edited form as:
Acta Biomater. 2012 March ; 8(3): 1117–1124. doi:10.1016/j.actbio.2011.11.028.

Mineral coatings modulate β-TCP stability and enable growth factor binding and release

Darilis Suárez-González[a,1], **Jae Sung Lee**[b,1], **Sheeny K. Lan Levengood**[b], **Ray Vanderby Jr.**[a,b,c], and **William L. Murphy**[a,b,d,*]

[a]Materials Science Program, University of Wisconsin, Madison, WI 53706, USA [b]Department of Biomedical Engineering, University of Wisconsin, Madison, WI 53706, USA [c]Orthopedics and Rehabilitation, University of Wisconsin, Madison, WI 53706, USA [d]Collaborative Research Center, AO Foundation, Davos, Switzerland

Abstract

β-Tricalcium phosphate (β-TCP) is an attractive ceramic for bone tissue repair because of its similar composition to bone mineral and its osteoconductivity. However, compared with other ceramics β-TCP has a rapid and uncontrolled rate of degradation. In the current study β-TCP granules were mineral coated with the aim of influencing the dissolution rate of β-TCP, and also to use the coating as a carrier for controlled release of the growth factors recombinant human vascular endothelial growth factor (rhVEGF), modular VEGF peptide (mVEGF), and modular bone morphogenetic protein 2 peptide (mBMP2). The biomineral coatings were formed by heterogeneous nucleation in aqueous solution using simulated body fluid solutions with varying concentrations of bicarbonate (HCO_3). Our results demonstrate that we could coat β-TCP granules with mineral layers possessing different dissolution properties. The presence of a biomineral coating delays the dissolution rate of the β-TCP granules. As the carbonate (CO_3^{2-}) content in the coating was increased the dissolution rate of the coated β-TCP also increased, but remained slower than the dissolution of uncoated β-TCP. In addition, we showed sustained release of multiple growth factors, with release kinetics that were controllable by varying the identity of the growth factor or the CO_3^{2-} con-tent in the mineral coating. Released rhVEGF induced human umbilical vein endothelial cell (HUVEC) proliferation, and mVEGF enhanced migration of mouse embryonic endothelial cells in a scratch wound healing assay, indicating that each released growth factor was biologically active.

Keywords

β-TCP; Bone morphogenetic protein 2; Vascular endothelial growth factor; Bone tissue engineering; Hydroxyapatite

1. Introduction

Calcium phosphate bioceramics are attractive materials for bone tissue repair because of their similar composition to bone mineral, good osteoconductivity (e.g. ability of a material to promote bone formation directly on their surfaces), and osteointegration (e.g. the ability

*Corresponding author at: Department of Biomedical Engineering, University of Wisconsin, Madison, WI 53706, USA. Tel.: +1 608 262 2224; fax: +1 608 265 9239. wlmurphy@wisc.edu (W.L. Murphy). .
[1]The first two authors contributed equally to this work.

to physically and chemically bond to the surface of bone tissue) [1,2]. The most widely used bioceramics are hydroxyapatite (HAP) and β-tricalcium phosphate (β-TCP), and these bioceramics have different physico-chemical properties as a result of their different compositions and crystalline structures. Both materials have been used as bone replacement materials. However, dense HAP is resorbed very slowly, if at all [3], while β-TCP has a relatively fast rate of degradation [4]. Controlled dissolution of bioceramics is a critical parameter in the design of bone tissue engineering scaffolds, as ideally the scaffold is replaced by bone as it degrades. In this regard, β-TCP can be characterized by an adversely high dissolution rate in some applications, while stoichiometric HAP is characterized by adversely low dissolution, which can result in incomplete resorption [3]. In the current study β-TCP granules were mineral coated with the aim of enhancing and controlling the dissolution rate of β-TCP.

Calcium phosphate bioceramics can also serve as carriers for growth factors due to their high affinity for proteins [5-7]. Growth factors can be surface bound or added as a powder during the formation of low temperature calcium phosphate cements [8]. Additionally, proteins have been co-precipitated during “biomimetic” growth of HAP coatings in simulated body fluids (SBF) to achieve sustained release as the biomineral is resorbed [9]. Several growth factors that influence bone formation have been released from HAP, including BMP2, TGFβ1, IGF1, and FGF2. However, since some calcium phosphate materials are rapidly resorbed while others are only slowly resorbed, growth factor release kinetics from a given bioceramic material are difficult to control. In this study we present an approach in which growth factors are bound to the surface of biomineral coatings, and the growth factor–biomineral affinity and intrinsic biomineral coating stability are varied. We hypothesized that varying the biomineral coating properties would result in different protein–biomineral interactions and biomineral dissolution rates, and therefore distinct release kinetics. We further hypothesized that this approach could be used to achieve different growth factor release profiles from the same carrier, which may be particularly important when trying to induce multiple processes essential to tissue repair. For example, angiogenesis and osteogenesis processes occur over relatively short (~2 weeks) and relatively long (>4–6 weeks) timeframes post fracture, respectively [10], and these processes are likely to benefit from distinct growth factor release timeframes.

Our approach to forming biomineral coatings mimics some aspects of natural biomineralization [11]. Specifically, coatings were nucleated and grown on a template material by incubation in solutions that approximate the ionic constituents, pH, and temperature of blood plasma, often termed simulated body fluids (SBF). This approach, initially established by Kokubo and co-workers [11], has been successfully used by us and others to nucleate resorbable HAP coatings on a variety of template materials, including glasses [12], metals [13], and polymers [14-17]. Because the biomineral is nucleated from an aqueous solution this technique can be applied to devices with complex porous geometries. In this study we propose to modulate the dissolution rate of HAP coatings by including impurities in the coatings in a controlled manner. In biological apatites impurities such as carbonate (CO_3^{2-}) ions tend to increase mineral solubility in comparison with pure stoichiometric HAP [18]. Therefore, we hypothesized that the biomineral coatings grown in SBF with varying HCO_3^- concentrations (4.2–100 mM) would result in coatings with different extents of CO_3^{2-} incorporation into the HAP mineral phase, which would in turn result in different dissolution rates. We further reasoned that these coatings could be used as a template for binding and controllable, sustained release of biologically active growth factors, including recombinant human vascular endothelial growth factor (rhVEGF), a modular peptide version of VEGF (mVEGF), and a modular peptide version of bone morphogenetic protein 2 (mBMP2). The engineered peptide growth factors contain a HAP-binding sequence inspired by the N-terminal α-helix of osteocalcin (OCN) [19] and a

biologically active sequence that mimics BMP2 [20,21] or rhVEGF [22]. The BMP2-mimicking peptide sequence has been previously shown by us to be biologically active [23]. Similarly, the VEGF-mimicking peptide has been shown to promote endothelial cell proliferation in vitro [22,24] and enhanced angiogenesis in vivo [25].

2. Materials and methods

2.1. β-TCP granules and incubation in mSBF with variations in HCO_3^- concentration

β-TCP granules and discs were obtained from Berkeley Advanced Biomaterials Inc. (Berkeley, CA). The granule size ranged from 3 to 6 mm. The discs had a diameter of 8 mm and a thickness of 3 mm. They were incubated at 37 °C in modified simulated body fluids (mSBF) with 4.2, 25 or 100 mM HCO_3 for a period of 14 days under continuous rotation. Each granule was incubated in 15 ml of mSBF. The mSBF solution had a similar composition to that of human plasma but with double the concentration of calcium and phosphate to enhance mineral growth, and was prepared as previously reported [17]. Specifically, the following reagents were added to deionized water heated to 37 °C in the order shown: 141 mM NaCl, 4.0 mM KCl, 0.5 mM $MgSO_4$, 1.0 mM $MgCl_2$, 4.2 or 100 mM $NaHCO_3$, 20.0 mM HEPES, 5.0 mM $CaCl_2$, and 2.0 mM KH_2PO_4. The solution was then adjusted to a final pH of 6.8. The mSBF solution was renewed daily.

2.2. Analysis of biomineral growth

2.2.1. Electron microscopy—β-TCP discs were used for the analysis of biomineral growth. The surface morphology of the biomineral coating was investigated by scanning electron microscopy (SEM). β-TCP discs incubated for 14 days were mounted on aluminum stubs and sputter coated with a thin layer of gold. Samples were imaged under high vacuum using a JEOL JSM-6100 scanning electron microscope operating at 10 keV.

2.2.2. FTIR spectroscopy—Fourier transform infrared (FTIR) spectroscopy was performed to identify the functional groups in the biomineral coating. Biomineral layers scraped from the surface of biomineral-coated discs were mixed with potassium bromide, pelletized, and recorded in the range 400–2000 cm^{-1} in transmission mode using an Equinox 55 spectrometer (Bruker AXS, Germany).

2.3. Biomineral stability

The stability of the β-TCP granules with or without a mineral coating was investigated by measuring the amount of calcium released into phosphate-buffered saline (PBS) using a colorimetric assay [26]. In brief, following mSBF incubation three β-TCP granules with a mass of 400 ± 1.5 mg were incubated in a 24-well plate at 37 °C in 1 ml of PBS. The PBS solution was collected on days 1, 2, 3, 5, 7, 10, 15, 21, and 30. Each time the buffer was replenished with fresh PBS. A total of 4 wells per coating condition were used for the dissolution experiments. To quantify the amount of calcium, 5 μl of sample was mixed with 195 μl of a 0.4 mM Arsenazo III/0.02 M Tris buffer solution at pH 7.4. The amount of calcium was quantitatively detected by measuring the absorbance at 615 nm using a BioTek Synergy plate reader and comparing it with a set of standards with known calcium concentrations. All data were normalized to the average mass of granules used (e.g. 400 mg).

2.4. Binding and release of rhVEGF and mVEGF

Radiolabeled rhVEGF or fluorescently tagged mVEGF were used for the release studies. ^{125}I-labeled rhVEGF was purchased from Perkin Elmer (Boston, MA). mVEGF was synthesized manually by solid phase peptide synthesis on Fmoc-Rink Amide MBHA resin

with Fmoc-protected α-amino acids with HOBT/DIC activation, as reported previously [24], and fluorescently active carboxyfluorescein was tagged on the N-terminus of mVEGF as needed. Each β-TCP granule was incubated in 250 μl of either VEGF solution (1 μg ml^{-1}, 0.35% ^{125}I-labeled rhVEGF; 500 μg ml^{-1} carboxyfluorescein-labeled mVEGF) at 37 °C for 1 h to allow equilibrium binding. The β-TCP granule was then transferred and incubated in 250 μl of Dulbecco's modified Eagle's medium (DMEM) at 37 °C. The radioactivity or the fluorescence intensity of the solution used for binding was measured to determine the percentage of growth factor initially bound. At the indicated time points the radioactivity or fluorescence intensity of the release medium was measured using a Packard Cobra II Gamma Counter (Meriden, CT) and a Bio-Tek Synergy plate reader (excitation/emission 494/519 nm), respectively. The fraction of rhVEGF in its native conformation after binding and release was quantified using a modified immuno-assay (R&D Systems, Minneapolis, MN) in which rhVEGF binding to rhVEGF-specific antibodies is dependent upon rhVEGF maintaining its native conformation. The mass of rhVEGF that bound during the immunoassay was normalized to the mass of released VEGF measured using the ^{125}I-rhVEGF radiotracer.

2.5. rhVEGF-induced cell proliferation

To confirm the release of biologically active rhVEGF we studied human umbilical vein endothelial cell (HUVEC) proliferation. HU-VEC were purchased from Lonza (Walkersville, MD). HUVEC were seeded in gelatin-coated 24-well plates at 11,000 cells per well using Medium 199 supplemented with the EGM-2 bullet kit (Lonza). Cells were allowed to attach overnight. The culture medium was changed to Medium 199 with 10% fetal bovine serum (Hy-Clone, Logan, UT). Transwell inserts (Corning, Corning, NJ) were placed in the wells in order to separate the β-TCP granules from the cells. β-TCP granules were autoclaved for sterilization prior to in vitro proliferation assay. Each sterile granule was incubated in 250 μl of rhVEGF solution (1 μg ml^{-1}) at 37 °C for 1 h and then rinsed in deionized H_2O. Five β-TCP granules were added per insert and medium added to give a total of 2 ml per well. The cells were allowed to proliferate for 72 h. Cell number was determined using the CellTiter-Blue Cell Viability Assay (Promega, Madison, WI).

2.6. mVEGF-induced cell migration

C166-GFP mouse endothelial cells (ATCC, Rockville, MD) were cultured in DMEM supplemented with 5% cosmic calf serum and a mixture of penicillin (100 U ml^{-1}), streptomycin (100 mg ml^{-1}) and G418 (0.2 mg ml^{-1}) at 37 °C in 5% CO_2. A scratch wound healing assay was performed to assess the effect of mVEGF on endothelial C166-GFP cell migration. Each scratch was created using a plastic pipette tip on a confluent cell layer in a 24-well plate well. After rinsing with PBS the cells were cultured under normal conditions in the presence of mVEGF-releasing granules or mVEGF-free granules placed in a transwell insert.

2.7. Binding and release of mBMP2

mBMP2 was synthesized manually by solid phase peptide synthesis on Fmoc-Rink Amide MBHA resin with Fmoc-protected α-amino groups with PyBop/DIPEA/HOBT activation, as previously reported [19]. Each β-TCP granule was incubated in 250 μl of carboxyfluorescein-labeled mBMP2 solution (0.5 mg ml^{-1}) at 37 °C for 1 h. The β-TCP granule was then rinsed with deionized water and transferred to and incubated in 250 μl of DMEM at 37 °C. At the indicated time points the release medium was collected and replaced with fresh medium. The amount of peptide released was measured as the fluorescence intensity of the release medium (excitation/emission 494/519 nm) using a BioTek Synergy plate reader.

2.8. Statistical analysis

All results are expressed as means ± standard deviations. Differences between data sets were assessed by an analysis of variance (ANOVA). A *P* value of less than 0.05 was considered significant.

3. Results

3.1. Characterization of biomineral coatings

Incubation of β-TCP discs in mSBF solutions with increasing carbonate concentrations resulted in the formation of biomineral coatings with apparently different morphologies. SEM micrographs confirmed the formation of a continuous biomineral coating after incubation for 7 days (Fig. 1a–c). A qualitative analysis based on SEM clearly demonstrated morphological differences resulting from using SBF solutions with different carbonate concentrations (Fig. 1d–f). The biomineral formed at lower carbonate concentrations primarily displayed a plate-like nanostructure (Fig. 1d), and the nanoscale plates became smaller as the carbonate concentration was increased (Fig. 1e and f). Fig. 1g shows the surface of the β-TCP discs before incubation.

FTIR analysis confirmed the incorporation of carbonate into the HAP coating (Fig. 2). The FTIR spectra showed two dominant peaks that can be attributed to O–P–O bending and asymmetrical P–O stretch of the PO_4^{3-} group of HAP (~600 and ~1100 cm^{-1}, respectively). The vibration peaks at 1500–1600 and ~880 cm^{-1}, which can be assigned to the carbonate (CO_3^{2-}) group, were more strongly detected in biomineral coatings formed in mSBF with 100 mM HCO_3 compared with those in 4.2 mM HCO_3 mSBF. As expected, our control group (no incubation) did not show a CO_3^{2-} peak, as CO_3^{2-} is not present in pure β-TCP. Thus carbonate incorporation into biomineral coatings was enhanced at higher carbonate concentrations in mSBF. CO_3^{2-} bands in this spectrum (at ~880 and 1500 cm^{-1}) indicate that the two common types of carbonate substitution (type A substitution for OH^- and type B substitution for PO_4^{3-}) are present in this compound [27].

HAP-coated samples with different extents of carbonate substitution had different dissolution characteristics in PBS. At higher levels of carbonate incorporation the rate of calcium release and the total amount of calcium release, both measures of biomineral dissolution, increased (Fig. 3). Importantly, the presence of the HAP biomineral coating decreased dissolution of β-TCP granules, as the uncoated granules exhibited the fastest dissolution rate.

3.2. Binding and sustained release of rhVEGF, mVEGF, and mBMP2

Multiple distinct growth factors could be bound to biomineral-coated β-TCP. The percentage of rhVEGF that bound to carbonated HAP with low carbonate substitution ($cHAP_{lowCO_3}$) coatings was 22 ± 6% in a solution containing 1 μg ml^{-1} rhVEGF (Fig. 4a). Binding efficiencies of mVEGF to $cHAP_{lowCO_3}$, to $cHAP_{midCO_3}$, and $cHAP_{high\ CO_3}$ were 87 ± 1.8%, 86 ± 2.2%, and 84 ± 1.9%, respectively (Fig. 4c). mBMP2 bound to these coatings with binding efficiencies of 94 ± 1.1%, 92.4 ± 0.6%, and 92.8 ± 0.7% (Fig. 5b). Thus the binding efficiencies for mBMP2 and mVEGF were similar, and were significantly higher than the rhVEGF binding efficiency.

Growth factors bound to biomineral-coated β-TCP were released in a sustained manner, and the release kinetics were dependent on the identity of the growth factor and the dissolution characteristics of the biomineral coating. rhVEGF released from biomineral-coated β-TCP was sustained over a 2 week period (Fig. 4b), including an initial burst release of 55 ± 10% during the first 3 days (Fig. 4b). Release of mVEGF was sustained for over 30 days from all

coatings and did not show a burst release. By day 3 only 0.6 ± 0.2%, 1 ± 0.1%, and 1 ± 0.1% mVEGF was released from $cHAP_{low\ CO_3}$, $cHAP_{mid\ CO_3}$, and $cHAP_{high\ CO_3}$, respectively (Fig. 4d). On day 30 1.9 ± 0.4%, 2.3 ± 0.4%, and 3.0 ± 0.6% of the mVEGF initially bound was released from $cHAP_{low\ CO_3}$, $cHAP_{mid\ CO_3}$, and $cHAP_{high\ CO_3}$, respectively (Fig. 4d). Similarly to mVEGF, the release of mBMP2 from biomineral-coated granules showed a minimal burst release and sustained release kinetics over extended periods of time (6 weeks), and the release kinetics were influenced by the characteristics of the biomineral coating (Fig. 5a and b). In particular, the rate and magnitude of mBMP2 release increased with increasing carbonate substitution in the coatings, which correlated with the biomineral dissolution data (Fig. 3). The mBMP2 released from $cHAP_{high\ CO_3}$ showed higher rates and a total release of approximate 70% of the bound growth factor compared to mBMP2 released from $cHAP_{low\ HCO_3}$. As the carbonate concentration in the biomineral coating decreased the percentage release de-creased from 70% from $cHAP_{high\ CO_3}$, to 50% from $cHAP_{mid\ HCO_3}$, to 25% from $cHAP_{low\ HCO_3}$.

3.3. Biological activity of rhVEGF

rhVEGF released from β-TCP was capable of binding to anti-VEGF antibody and was capable of promoting HUVEC proliferation. As an initial demonstration of biological activity we evaluated rhVEGF released using an ELISA. We first determined that 83 ± 23% rhVEGF in the stock solution was detected via ELISA (data not shown). We used that value as an indication of the maximum amount of rhVEGF that could bind to the anti-VEGF antibody, which was used to normalize the amount of antibody-reactive rhVEGF released (a preliminary measure of biological activity). Our results show that 80 ± 13% and 82 ± 32% of the released rhVEGF was ELISA-reactive on days 1 and 2, respectively. The amount of ELISA-reactive VEGF then decreased to 39 ± 15% and 29 ± 4% on days 3 and 7, respectively (Fig. 6). In addition, we evaluated whether the released rhVEGF was capable of promoting HU-VEC proliferation, a well-defined measure of rhVEGF biological activity. HUVEC proliferation was significantly higher in the pres-ence of rhVEGF, whether the rhVEGF was added as a bolus or released from biomineral-coated β-TCP. The group that was releasing rhVEGF from biomineral-coated β-TCP showed no significant difference in HUVEC metabolic activity compared with the group receiving bolus rhVEGF during the 72 h incubation period evaluated (Fig. 7). These data demonstrate that the released rhVEGF was as biologically active as the rhVEGF added as a bolus to the cell culture medium. Interestingly, VEGF-induced HUVEC proliferation required a lower concentration of released rhVEGF when compared with bolus rhVEGF. Specifically, based on the release profiles of rhVEGF (Fig. 4a), the amount of rhVEGF released into the cell culture medium was approximately 0.5 ng ml^{-1}, which is 2-fold lower than the 1 ng ml^{-1} concentration that was used in the bolus administration of rhVEGF. The metabolic activity of the groups receiving rhVEGF showed a 2-fold increase compared with the group that was incubated with β-TCP granules that were not releasing rhVEGF.

mVEGF released from mineral coated β-TCP enhanced the migration of C166-GFP mouse endothelial cells in a scratch wound healing assay in vitro. A significant enhancement of cell migration into a scratch wound was observed in the mVEGF-coated group compared with the uncoated group (mineral-coated β-TCP)(Fig. 8). Interestingly, migration in the uncoated group was also enhanced compared with the control group (no β-TCP), suggesting that ions released from mineral-coated β-TCP may positively influence endothelial cell activity in the absence of rhVEGF or mVEGF.

4. Discussion

Incubation of β-TCP in mSBF solutions with increasing carbon-ate concentrations resulted in the formation of a continuous mineral layer with different morphological features (Fig.

1a–g). Formation of the mineral coating probably involved the interaction of the calcium and phosphate ions in solution with the calcium and phosphate groups in β-TCP, the formation of HAP nuclei on the surface, and subsequent growth of these nuclei to form a continuous coating, as described in analogous approaches previously[2,28,29]. The plates in the plate-like nanostructure in the coating became smaller as carbonate substitution increased. Ionic substitution is known to disrupt the structure and lattice of the mineral formed, and an increase in carbonate substitution has been shown to result in decreased apatite crystallinity [28,30,31]. The presence of the mineral coating dramatically decreased the dissolution of β-TCP biomaterials. This is a potentially important result, as β-TCP ceramics are known to be less stable than other common bioceramics, and may be resorbed more quickly than desired for some clinical applications. In particular, β-TCP granules have been shown to degrade 3–12 times faster than HAP in vitro, depending on experimental variables such as the buffer used and the granule size [2]. In vivo β-TCP can take between 4 and 16 months to degrade[32,33], whereas HAP can remain for over 5 years post-surgery without evidence of substantial resorption [32]. Therefore, in some clinical applications there is a need to decrease the dissolution rate of β-TCP so that it remains present during the time course of new bone formation (several months), but to avoid the lack of resorption observed in more stable bioceramics such as HAP. The solubility characteristics of the coatings in aqueous buffer varied, with different dissolution rates among the coatings with different extents of carbonate substitution. Thus our results show that at higher carbonate concentrations the rate and total amount of calcium release increased, and varying the degree of carbonate incorporation resulted in a modulation of the dissolution kinetics (Fig. 3).

The solubility of apatites is affected by the extent of ionic substitution in the apatite lattice, and also by the crystallinity of the mineral [31]. Carbonate substitution has been shown to increase the solubility of apatites [18,31,34]. Similarly, the degree of crystallinity affects the solubility of apatites. Highly crystalline apatites tend to be insoluble, while poorly crystalline apatites have higher relative solubilities. With the formation of a mineral coating on β-TCP we can modulate its dissolution rate, and potentially match the bioceramic resorption with the intended end goal, whether the end goal is short-term (e.g. drug delivery) or longer term (e.g. bone reconstruction and replacement).

The mineral coating served as a simple and highly adaptable carrier to bind and release rhVEGF, mVEGF, and mBMP2. The surface of the mineral coating is highly porous and contains charged calcium and phosphate components. Therefore, we hypothesized that the coating would be capable of binding growth factors via electrostatic interactions, and that the growth factors would be released at different rates based on the affinity of the growth factor for the mineral coating and the dynamics of coating dissolution. Analysis of the release profiles of the growth factors from mineral-coated β-TCP biomaterials showed that: (1) the affinity of the growth factor could be enhanced by incorporating a mineral binding sequence into the growth factor, resulting in a higher binding efficiency and longer term release; (2) the dynamics of coating dissolution influence growth factor release, with higher dissolution rates leading to more rapid release. In particular, the rhVEGF and mVEGF release data demonstrate the ability to vary the growth factor release profile based on the growth factor-coating affinity, as mVEGF is designed to have a higher mineral-binding affinity than rhVEGF. As expected, rhVEGF was released in the short term (with-in 2 weeks), while mVEGF was released over more than 4 weeks (Fig. 4b and d). In addition, both the mBMP2 release data and the mVEGF release data demonstrate the ability to control the release kinetics by modulating the coating dissolution rate. The mBMP2 and mVEGF release kinetics were directly related to the extent of carbonate substitution in the mineral coating (Figs. 4b and 5a), which indicates that the growth factor release rate is correlated with coating dissolution. The ability to modulate the growth factor release kinetics via two

separate mechanisms (growth factor–coating affinity and coating dissolution) is potentially useful in bone tissue engineering, as it is desirable to be able to tailor the growth factor release kinetics to suit the particular growth factor and the intended clinical indication. For example, rhVEGF influences blood vessel formation early during fracture repair. Therefore, short-term release of rhVEGF would be preferred in bone repair applications. In contrast, long-term release of BMP2 is likely to be more advantageous to stimulate and sustain tissue regeneration. BMP2 has been shown to enhance bone regeneration in critical sized segmental bone defects in long-term studies (over 8 weeks) [35,36], and Jeon et al. demonstrated that long-term delivery of BMP2 enhances its in vivo osteogenic efficacy [37]. Current clinical approaches to growth factor delivery involve including proteins within a collagen sponge. Despite the early clinical success of bone growth factor delivery, there are significant limitations. For example, the release kinetics of rhBMP2 from collagen sponges exhibits a burst release over the first 4 days after implantation, resulting in short term release. Growth factors can also diffuse from materials and/or be degraded rapidly in vivo, resulting in limited bioavailability. The methods presented in this study for growth factor binding and release represent a simple approach that could be easily translated to a clinical setting and allow sustained, controllable release kinetics.

rhVEGF released from the β-TCP biomaterials promoted proliferation of HUVEC, which demonstrates that the biological activity of rhVEGF was not substantially compromised during binding and release. Over 80% of the rhVEGF released within the first 2 days is capable of binding to an anti-rhVEGF antibody and therefore is likely to be in its native conformation (Fig. 5). That percentage decreased over time to 39% on day 3 and 29% on day 7, by which time most of the initially bound rhVEGF was released (77%). However, incubation of HUVEC with mineral-coated biomaterials releasing rhVEGF enhanced their proliferation compared with the group that did not receive rhVEGF, indicating that the percentage of rhVEGF remaining active after release was high enough to cause a biological response. rhVEGF is not highly stable in biological solutions, and has a half-life of the order of hours (~8 h) in cell culture medium [38]. In vivo rhVEGF is bound by proteins such as HuR, which inhibit its degradation and can increase the rhVEGF half-life 3- to 8-fold [38,39]. The absence of these proteins in our in vitro characterization work could have influenced the decreased observed in the percentage of rhVEGF that was ELISA-reactive (Fig. 5). mVEGF significantly enhanced migration of C166 mouse endothelial cells compared with the condition without β-TCP and that with β-TCP alone, indicating that the mVEGF was biologically active (Fig. 8). This result is consistent with previous studies, in which we have demonstrated biological activity of mVEGF [24]. The more general observation of modular peptide biological activity is also consistent with our previous demonstration of mBMP2 biological activity [19]. Interestingly, β-TCP alone resulted in enhanced scratch wound healing, which suggests that a component released from β-TCP may positively influence endothelial cell migration and/or proliferation. Further studies will be required to delineate specific β-TCP-derived factors that may influence endothelial cell signaling.

5. Conclusion

In this study we have demonstrated that the dissolution rate of mineral-coated β-TCP can be modulated by varying carbonate incorporation into the mineral coating. We have also demonstrated that the mineral coating can be used as an efficient and controllable template for growth factor binding and release. This approach to mineral coating can be applied to a variety of template materials and geometries, and the growth factor incorporation process represents a simple technique that may be easily incorporated into clinical settings.

Acknowledgments

The authors acknowledge funding from the AO Research Foundation (Focus Grant No. F-07-65M), a pre-doctoral fellowship from the Harriet Jenkins Pre-Doctoral Fellowship Program (DS), and a T32 Training Grant (T32 DC009401).

Appendix A. Figures with essential colour discrimination

Certain figures in this article, particularly Figures 7 and 8, are difficult to interpret in black and white. The full colour images can be found in the on-line version, at doi:10.1016/j.actbio.2011.11.028.

References

[1]. Mayr HO, Dietrich M, Fraedrich F, Hube R, Nerlich A, von Eisenhart-Rothe R, et al. Microporous pure beta-tricalcium phosphate implants for press-fit fixation of anterior cruciate ligament grafts: strength and healing in a sheep model. Arthroscopy. 2009; 25(9):996–1005. [PubMed: 19732638]

[2]. LeGeros RZ. Biodegradation and bioresorption of calcium phosphate ceramics. Clin Mater. 1993; 14(1):65–88. [PubMed: 10171998]

[3]. Mastrogiacomo M, Corsi A, Francioso E, Di Comite M, Monetti F, Scaglione S, et al. Reconstruction of extensive long bone defects in sheep using resorbable bioceramics based on silicon stabilized tricalcium phosphate. Tissue Eng. 2006; 12(5):1261–73. [PubMed: 16771639]

[4]. Tang R. Kinetics of dissolution of b-tricalcium phosphate. Langmuir. 2001; 17:3480–5.

[5]. Schroder E, Jonsson T, Poole L. Hydroxyapatite chromatography: altering the phosphate-dependent elution profile of protein as a function of pH. Anal Biochem. 2003; 313(1):176–8. [PubMed: 12576076]

[6]. Alt V, Pfefferle HJ, Kreuter J, Stahl JP, Pavlidis T, Meyer C, et al. Effect of glycerol-l-lactide coating polymer on bone ingrowth of bFGF-coated hydroxyapatite implants. J Control Release. 2004; 99(1):103–11. [PubMed: 15342184]

[7]. Bernardi G, Kawasaki T. Chromatography of polypeptides and proteins on hydroxyapatite columns. Biochim Biophys Acta. 1968; 160(3):301–10. [PubMed: 5680264]

[8]. Issa JP, Bentley MV, Iyomasa MM, Sebald W, De Albuquerque RF. Sustained release carriers used to deliver bone morphogenetic proteins in the bone healing process. Anat Histol Embryol. 2008; 37(3):181–7. [PubMed: 18070240]

[9]. Lee JS, Suarez-Gonzalez D, Murphy WL. Mineral coatings for temporally controlled delivery of multiple proteins. Adv Mater. 2011; 23:4279–84. [PubMed: 22039597]

[10]. Simmons DJ. Fracture healing perspectives. Clin Orthop Relat Res. 1985; 200:100–13. [PubMed: 3905103]

[11]. Kokubo T, Kushitani H, Sakka S, Kitsugi T, Yamamuro T. Solutions able to reproduce in vivo surface-structure changes in bioactive glass-ceramic A-W. J Biomed Mater Res. 1990; 24(6): 721–34. [PubMed: 2361964]

[12]. Li P, Ohtsuki C, Kokubo T, Nakanishi K, Soga N, Nakamura T, et al. Apatite formation induced by silica gel in a simulated body fluid. J Am Ceram Soc. 1992; 75(8):2094–7.

[13]. Habibovic P. Biomimetic hydroxyapatite coating on metal implants. J Am Ceram Soc. 2002; 85(3):517–22.

[14]. Murphy WL, Mooney DJ. Bioinspired growth of crystalline carbonate apatite on biodegradable polymer substrata. J Am Chem Soc. 2002; 124(9):1910–7. [PubMed: 11866603]

[15]. Zhang R, Ma PX. Biomimetic polymer/apatite composite scaffolds for mineralized tissue engineering. Macromol Biosci. 2004; 4(2):100–11. [PubMed: 15468200]

[16]. Zhang Y, Ni M, Zhang M, Ratner B. Calcium phosphate–chitosan composite scaffolds for bone tissue engineering. Tissue Eng. 2003; 9(2):337–45. [PubMed: 12740096]

[17]. Suarez-Gonzalez D, Barnhart K, Saito E, Vanderby R Jr, Hollister SJ, Murphy WL. Controlled nucleation of hydroxyapatite on alginate scaffolds for stem cell-based bone tissue engineering. J Biomed Mater Res A. 2010; 95(1):222–34. [PubMed: 20574984]

[18]. Haobo Pan BWD. Effect of carbonate on hydroxyapatite solubility. Cryst Growth Des. 2010; 10(2):845–50.

[19]. Lee JS, Lee JS, Murphy WL. Modular peptides promote human mesenchymal stem cell differentiation on biomaterial surfaces. Acta Biomater. 2010; 6(1):21–8. [PubMed: 19665062]

[20]. Saito A, Suzuki Y, Kitamura M, Ogata S, Yoshihara Y, Masuda S, et al. Repair of 20-mm long rabbit radial bone defects using BMP-derived peptide combined with an alpha-tricalcium phosphate scaffold. J Biomed Mater Res A. 2006; 77(4):700–6. [PubMed: 16550532]

[21]. Saito A, Suzuki Y, Ogata S, Ohtsuki C, Tanihara M. Prolonged ectopic calcification induced by BMP-2-derived synthetic peptide. J Biomed Mater Res A. 2004; 70(1):115–21. [PubMed: 15174115]

[22]. D'Andrea LD, Iaccarino G, Fattorusso R, Sorriento D, Carannante C, Capasso D, et al. Targeting angiogenesis: structural characterization and biological properties of a de novo engineered VEGF mimicking peptide. Proc Natl Acad Sci USA. 2005; 102(40):14215–20. [PubMed: 16186493]

[23]. Lu Y, Markel MD, Nemke B, Lee JS, Graf BK, Murphy WL. Influence of hydroxyapatite-coated and growth factor-releasing interference screws on tendon–bone healing in an ovine model. Arthroscopy. 2009; 25(12):1427e1–34e1. [PubMed: 19962070]

[24]. Lee JS, Wagoner Johnson AJ, Murphy WL. A modular, hydroxyapatite-binding version of vascular endothelial growth factor. Adv Mater. 2010; 22(48):5494–8. [PubMed: 20941802]

[25]. Santulli G, Ciccarelli M, Palumbo G, Campanile A, Galasso G, Ziaco B, et al. In vivo properties of the proangiogenic peptide QK. J Transl Med. 2009; 7:41. [PubMed: 19505323]

[26]. William L, Murphy PBM. Compartmental control of mineral formation: adaptation of a biomineralization strategy for biomedical use. Polyhedron. 2000; 19:357–63.

[27]. Santos M. A model for B carbonate apatite. Inorg Chem. 1977; 16(8):2131–4.

[28]. Blumenthal NC, Betts F, Posner AS. Effect of carbonate and biological macromolecules on formation and properties of hydroxyapatite. Calcif Tissue Res. 1975; 18(2):81–90. [PubMed: 1148899]

[29]. Suarez-Gonzalez DBK, Migneco F, Flanagan C, Hollister SJ, Murphy WL. Controllable mineral coatings on PCL scaffolds as carriers for growth factor release. Biomaterials. 2012; 33:713–21. [PubMed: 22014948]

[30]. Barralet J, Best S, Bonfield W. Carbonate substitution in precipitated hydroxyapatite: an investigation into the effects of reaction temperature and bicarbonate ion concentration. J Biomed Mater Res. 1998; 41(1):79–86. [PubMed: 9641627]

[31]. Fulmer MT, Ison IC, Hankermayer CR, Constantz BR, Ross J. Measurements of the solubilities and dissolution rates of several hydroxyapatites. Biomaterials. 2002; 23(3):751–5. [PubMed: 11771695]

[32]. Quarto R, Mastrogiacomo M, Cancedda R, Kutepov SM, Mukhachev V, Lavroukov A, et al. Repair of large bone defects with the use of autologous bone marrow stromal cells. N Engl J Med. 2001; 344(5):385–6. [PubMed: 11195802]

[33]. Klein CP, de Groot K, Driessen AA, van der Lubbe HB. Interaction of biodegradable beta-whitlockite ceramics with bone tissue: an in vivo study. Biomaterials. 1985; 6(3):189–92. [PubMed: 4005363]

[34]. Haobo P. Apatite-formation ability – predictor of "bioactivity"? Acta Biomaterialia. 2010; 6:4181–8. [PubMed: 20493974]

[35]. Kolambkar YM, Dupont KM, Boerckel JD, Huebsch N, Mooney DJ, Hutmacher DW, et al. An alginate-based hybrid system for growth factor delivery in the functional repair of large bone defects. Biomaterials. 2011; 32(1):65–74. [PubMed: 20864165]

[36]. Edwards RB, Seeherman HJ, Bogdanske JJ, Devitt J, Vanderby R Jr, Markel MD. Percutaneous injection of recombinant human bone morphogenetic protein-2 in a calcium phosphate paste accelerates healing of a canine tibial osteotomy. J Bone Joint Surg Am. 2004; 86A(7):1425–38. [PubMed: 15252089]

[37]. Jeon O, Song SJ, Yang HS, Bhang SH, Kang SW, Sung MA, et al. Long-term delivery enhances in vivo osteogenic efficacy of bone morphogenetic protein-2 compared to short-term delivery. Biochem Biophys Res Commun. 2008; 369(2):774–80. [PubMed: 18313401]

[38]. Levy NS, Chung S, Furneaux H, Levy AP. Hypoxic stabilization of vascular endothelial growth factor mRNA by the RNA-binding protein HuR. J Biol Chem. 1998; 273(11):6417–23. [PubMed: 9497373]

[39]. Semenza GL. Regulation of hypoxia-induced angiogenesis: a chaperone escorts VEGF to the dance. J Clin Invest. 2001; 108(1):39–40. [PubMed: 11435455]

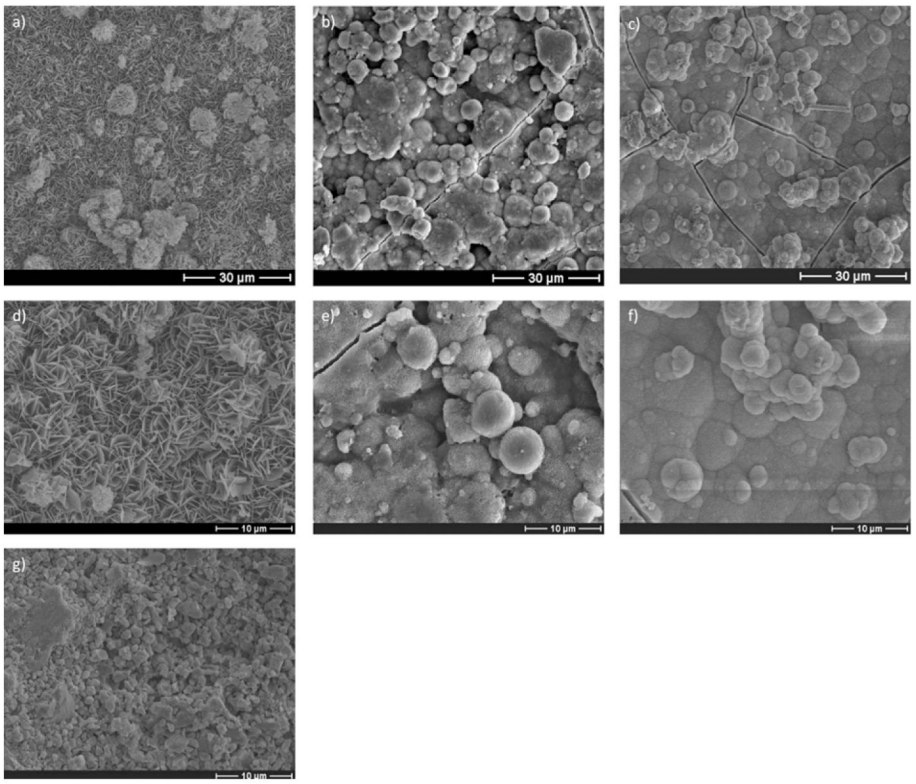

Fig. 1.

SEM micrographs of β-TCP discs after 14 days incubation in mSBF with a bicarbonate concentration of (a) 4.2, (b) 25, and (c) 100 mM HCO_3^- show the formation of a continuous coating. The morphology of the mineral is affected by the extent of carbonate substitution. The plate-like nanostructure at lower HCO_3^- in mSBF, (d) 4.2 mM, becomes smaller as the concentration of HCO_3^- in mSBF increases to (e) 25 and (f) 100 mM. (g) The surface before incubation in mSBF.

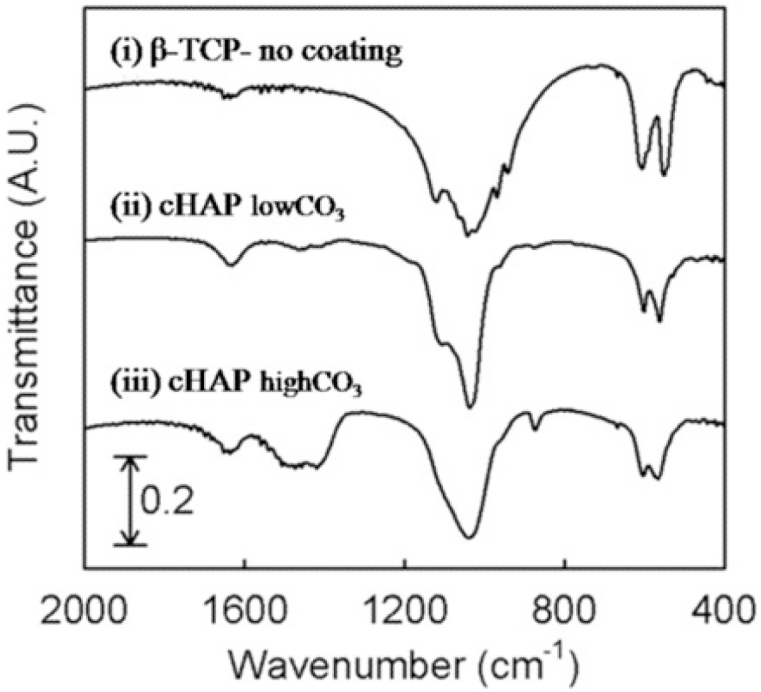

Fig. 2.

FTIR a spectrum of β-TCP discs before incubation in mSBF (i) and after incubation in mSBF with (ii) 4.2 ($cHAP_{low\ CO_3}$) or (iii) 100 mM HCO_3^-($cHAP_{high\ CO_3}$). The increased peak intensity at 1500–1600 cm^{-1} in (iii) compared with (i) indicates higher carbonation in the cHAP coating.

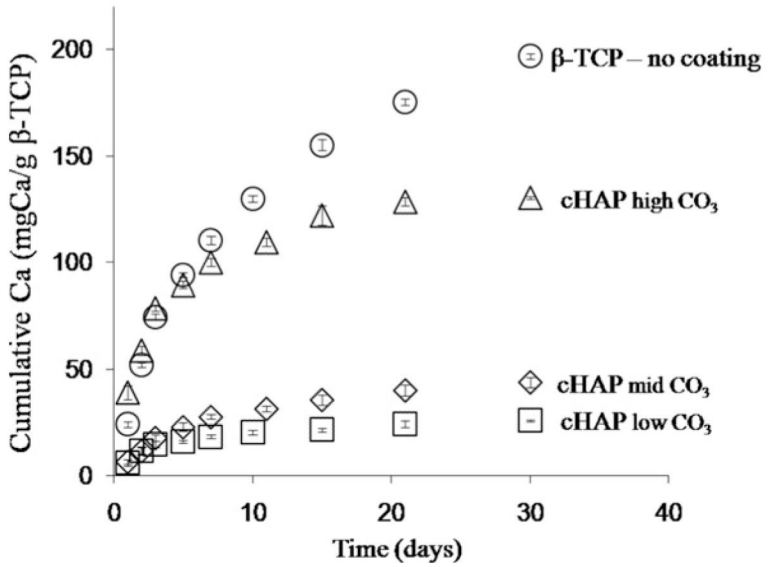

Fig. 3.

Stability of the β-TCP granules. Release of calcium ions from uncoated and coated granules after incubation in mSBF with 4.2, 25, and 100 mM HCO_3^- is represented by the circles, triangles, diamonds and rectangles, respectively. The presence of the mineral coating improves the stability of the β-TCP granules. In the mineral-coated groups as the HCO_3^- concentration in mSBF increased the rate of dissolution increased as well.

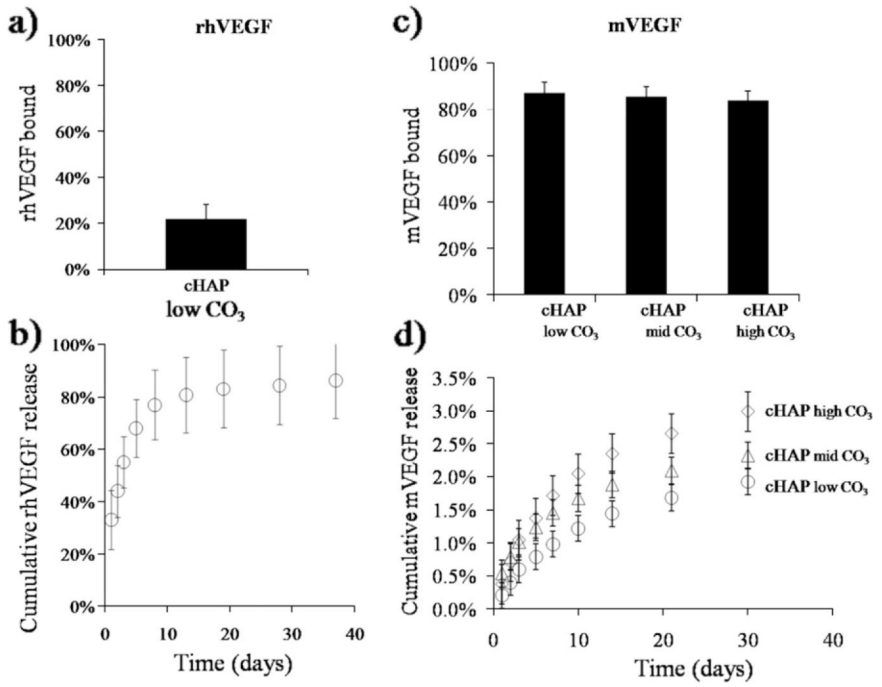

Fig. 4.

Binding of (a) rhVEGF and (b) mVEGF to biomineral-coated β-TPC. (a and c) Since mVEGF interacts more strongly with the mineral coating than rhVEGF due to the mineral binding sequence the percentage of mVEGF bound (>80%) to all coatings was higher compared with rhVEGF (22%). (b and d) Cumulative release of rhVEGF and mVEGF from mineral-coated β-TCP granules. rhVEGF was released during the first 10 days. In contrast, mVEGF was released over longer time frames.

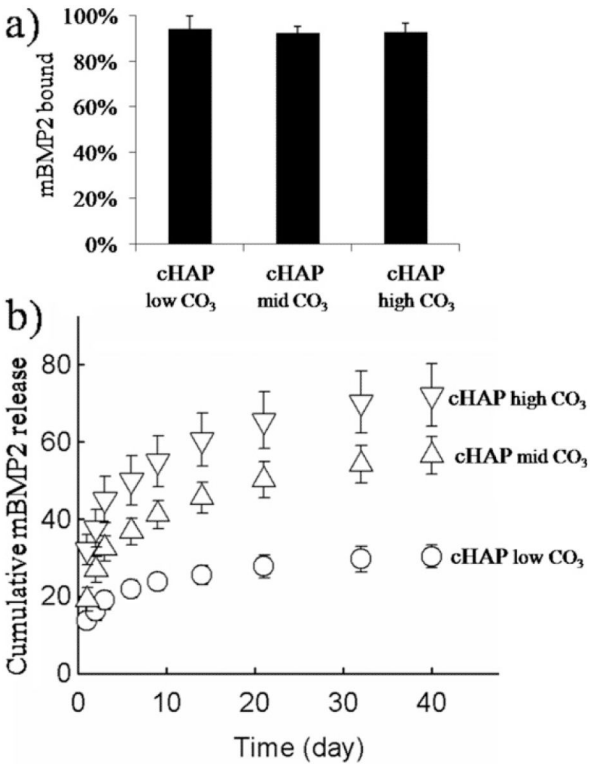

Fig. 5.

(a) mBMP2 bound with high affinity to the biomineral coating. The percentage of mBMP2 bound was not affected by the extent of carbonate substitution in the mineral coating. (b) Cumulative release of mBMP2 from the mineral coating formed on β-TCP granules by incubating in mSBF with different bicarbonate concentrations; ○, 4.2 mM; △, 25 mM; ▽, 100 mM. The release of mBMP2 correlated with the rate of dissolution of the mineral coating. At higher carbonate concentrations mBMP2 was released at higher rates.

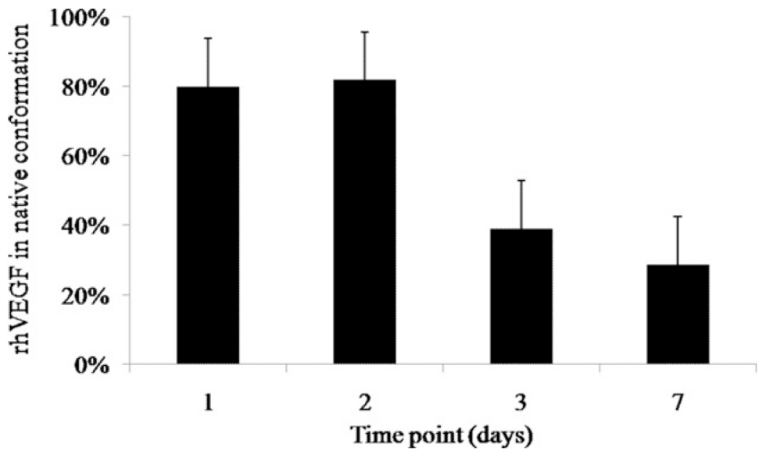

Fig. 6.
The fraction of rhVEGF that maintained its native conformation after release from β-TCP decreased over time.

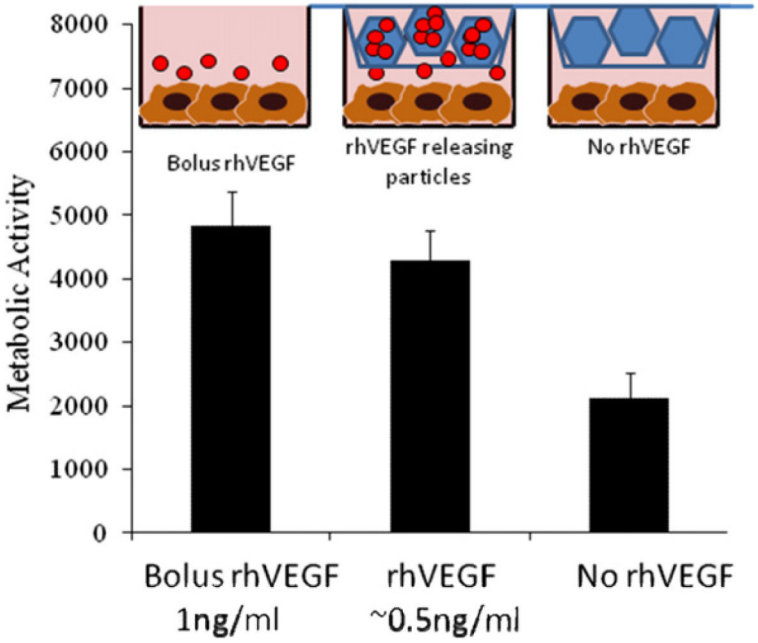

Fig. 7.

The release of rhVEGF from mineral-coated β-TCP granules significantly enhanced HUVEC proliferation, here measured using a blue cell titer assay (arbitrary units). There were no significant differences between bolus administration of rhVEGF and released rhVEGF, but, based on the release data, the concentration of rhVEGF from the slow release group was 0.5 ng ml^{-1}. In the group exposed to bolus rhVEGF the cells were exposed to 1 ng ml^{-1}. The granules releasing rhVEGF influenced proliferation at half the concentration of the bolus group.

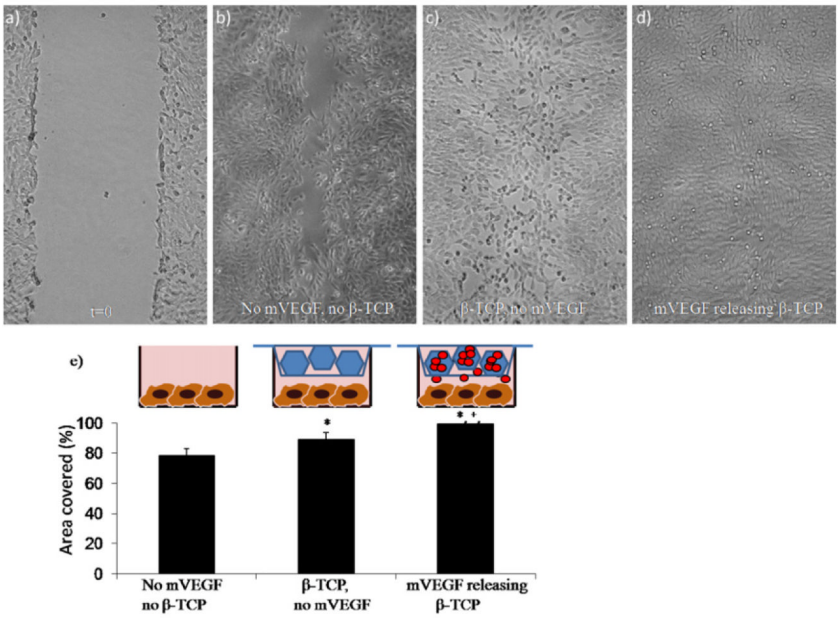

Fig. 8.

C166-GFP scratch wound healing assay. Optical microscopic images of a scratch: (a) immediately after scratch formation and after 14 h in culture (b) under normal conditions, (c) in the presence of mineralized TCP granules and (d) in the presence of mVEGF-coated, mineralized TCP granules. (e) Percentage of area covered after migration of cells for 14 h. *Significance compared with the no mVEGF, no β-TCP group; $^{+}$significance compared with the β-TCP, no mVEGF group.